Grid Forming Converters in Offshore Wind Farms for Grid Integration Through Hybrid HVDC Transmission System

Muhammad Waleed Raza*‡, Muhammad Raza*

*Department of Electrical Engineering, Bahria University Karachi Campus, 13, National Stadium Road, Karachi, Pakistan

(02-281191-002@student.bahria.edu.pk, mraza.bukc@bahria.edu.pk)

‡ Corresponding Author; Muhammad Waleed Raza, 13, National Stadium Road, Karachi, Pakistan, 02-281191-002@student.bahria.edu.pk

Received: 06.05.2022 Accepted: 16.06.2022

Abstract- For remote offshore wind farms, the diode rectifier unit (DRU) based HVDC system has received prominent interest. This is due to the fact that they provide higher efficiency, require a smaller footprint, high reliability, and lower costs. However, the problem with using DRU at the offshore substation is that they are unable to establish the offshore substation due to the absence of a voltage source. So, the wind turbine control system needs to change to grid forming (GFM) control instead of the conventional grid following (GFL) control. This control philosophy change is the main hindrance to the industrialization of the hybrid HVDC system. This paper proposes a novel GFM converter control based on the idea that the DC-link voltage can imply power differences similar to a synchronous machine frequency. To drive the converter frequency, the DC voltage, up to a certain constant factor, is used. Additionally, a nonlinear model is simulated in MATLAB/Simulink with the proposed and existing control techniques, and the results of simulations are compared. Furthermore, the proposed control technique is investigated for offshore wind farms. The proposed control technique is verified using simulation results in MATLAB/Simulink.

Keywords Hybrid HVDC System, Grid Forming Converter, Applications of Grid Forming Converters, Offshore Wind Farms, Frequency Control.

1. Introduction

As the world is looking for more green energy, offshore wind energy is becoming more popular. This usage of wind energy will reduce greenhouse gas emissions and reduce pollution. There are several challenges to transmitting offshore wind power economically and reliably to the onshore grid. Since HVDC transmissions are cheaper than HVAC transmissions for distances over 90 km, they are used for distances beyond 90 km [1], [2]. Electronic power converters are employed to convert this AC power to DC. The electronic power converters used for this conversion of power can be voltage source converter or modular multilevel converter or line commuted converter or the diode rectifier unit. With applications such as high voltage HVDC transmission, the MMC is becoming increasingly popular [3]. This is due to the technical advantages like providing independent active and reactive power control, grid forming (GFM) capability, and current control [4]. The hybrid HVDC system contains both a voltage source converter and a current source converter for the conversion of power and control of the system. Which type of power converter will be used onshore or offshore depends upon the topology and control. The current source converter especially the diode rectifier unit (DRU) based HVDC has received prominent interest for being used in remote offshore wind farms [4], [5]. This is due to the fact that they provide higher efficiency, require a smaller footprint, high reliability, and lower costs [6]. However, the problem in using DRU at the offshore substation is that they are unable to establish the offshore substation due to lack of voltage source. Another disadvantage is the need for reactive power is increased because the DRU cannot provide the reactive power. Offshore network equipment like a transformer needs to be energized and the reactive power compensation for the offshore network cables is need to be done by converters or capacitors available at offshore substation [7], [8]. Additionally, the DRU is unable to deliver startup power to wind turbine (WT) [7]. So, the wind turbine control system needs to change to GFM control instead of the conventional grid following (GFL) control [7], [9], [10]. This control philosophy change is the main hindrance to the industrialization of the hybrid HVDC system.

Multi-megawatt wind turbines are typically coupled with the power conversion systems to increase the efficiency of wind turbines and support grids under normal and abnormal operations. Controls of power conversion systems in multi-megawatt wind turbines for large wind farms will play an

essential role in improving the power system stability with high wind penetration.

Typical turbine controllers are based on the grid-following (GFL) techniques, in which the phase locked loop (PLL) is used to track the instantaneous angle of the point of common coupling (PCC) voltage, and the current control loop is used to regulate the AC current reflecting active and reactive power. The main issue in using PLL is that it negatively reduces the power converter stability's margin, especially when the grid condition is weak [11].

The instability of multi-megawatt wind turbines will result in more severe impacts on the overall power system stability. Grid-forming (GFM) controls can address the instability issues of wind turbines under weak grid conditions as they do not require the PLL [12]. A wind turbine with GFM control behaves as a controllable voltage source behind a low output impedance, which forms the voltage magnitude and frequency of the grid. Thus, the GFM wind turbines can operate independently from the main power grid and possesses the black start capability with a sufficient energy buffer. A successful trial of a recent 69 MW wind park operated in the GFM mode reveals GFM wind turbines' potential with additional promising inertia support and black start capability [13], [14].

Grid forming control was proposed in [5] for the very first time for a hybrid HVDC system containing DRU. The proposed centralized control scheme effectively maintained voltage and frequency at the offshore substation. Another GFM control was proposed in [15] which provided the WT synchronizing signal using a global positioning system (GPS). A decentralized GFM control based on distributed phase-locked loop (PLL) was presented in [16] which operated as a GFM control without needing any communication. In [4] a GFM control depending on the active power change is presented. The active power change is started by changing the angle of voltage of the WT converters. The main feature of this control was preventing reactive power swings among the WTs. However, the dynamics in each WTs dc link and behind it were not considered. A method to control the output power of the wind farm was proposed in [17]. It uses a fixed power strategy to remove ripples from the output power of the wind farm. This gives a smooth output of power.

Moreover, GFM converter technology is still a relatively new field. GFM converters lack knowledge of modeling techniques, control methodologies, challenges, and applications. The modern grid forming converters have limited usability in the offshore wind farms and diode rectifier-based hybrid HVDC systems where establishing a grid is the main problem. This article proposes a novel grid forming converter control for offshore WTs connected with a hybrid HVDC system. The proposed control uses the idea that the DC-link voltage can imply power disparities similar to a synchronous machine frequency. To drive the converter frequency, the DC voltage, up to a certain constant factor, is used. This converter control is used to establish the offshore network so other conventional grid following WTs can connect with the offshore network.

Additionally, the idea of using the GFM WTs with other conventional GFL WTs in hybrid HVDC system i.e. containing DRU at the offshore substation is fairly new. This paper investigates the use of GFM WTs along with conventional GFL WTs in a hybrid HVDC system. This proposed grid forming control can be extended to solve the persisting issues in the conventional hybrid HVDC systems and offshore wind farms.

1.1 Contributions

The main purpose of this article is to propose a type of GFM converter control that is suitable for a hybrid HVDC transmission system based on DRU. This article helps as a valuable resource for investigators beginning their learning on GFM converters and electrical power engineers discovering explanations to the evolving challenges. The major contributions of this paper are:

- A grid forming control technique is proposed based on the DC link voltage of the converter to export power to load through the voltage source converter.
- The proposed control technique is investigated in offshore wind farms.
- The proposed control is decentralized and requires neither communication nor any GPS signal.

As a summary, the article is comprised of the following sections: the second section presents a comprehensive review of grid forming converter control and its types. The overview of the model used and the detailed overview of the control proposed are given in section three. Section four compares different GFM control techniques with the proposed control method by simulation using MATLAB/Simulink and investigates the use of proposed control in offshore wind farms. The conclusion is given in the final section.

2 Literature Review

Controls for conventional wind turbine converters are designed to operate under the assumption that they are linked to an extremely strong grid. This means that the converter will follow an already existing voltage signal produced by an offshore converter working in voltage and frequency control mode [18]. This is called grid following control (GFL). The wind turbine should be capable of producing its own signal of voltage for reference purposes. This is commonly known as grid forming control (GFM) and is also called voltage injection control [19]. The use of GFM control reduces the dependency on diesel generators, which are employed at offshore power plants to deliver ancillary power required for energization. This improves the reliability of the wind power plant system offshore and also lowers its expense and size of it [18]. The basic concept of GFM converter is shown in Fig. 1.

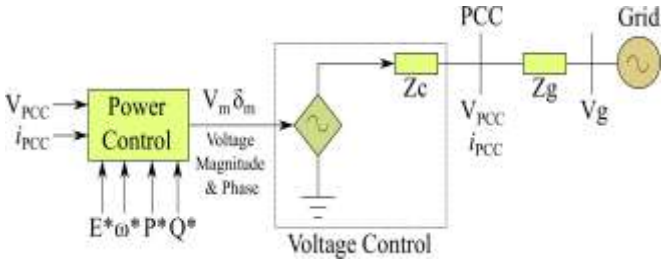

Fig. 1. Concept of grid forming control

In the conventional GFL control, the use of energy storage units is inevitable to provide frequency support [20]. The authors in [20] were able to compensate for imbalances during uncertainty by coordinating ocean renewable energy storage with offshore wind farms. However, in near-to-sea places, the construction of pumped storage is near to impossible. So, ocean renewable energy storage with offshore wind farms is preferred.

2.1. Types of Grid Forming Control

The most common control method for GFL converters is the control of current utilizing vectors. In opposition to this, the GFM converters have the capability to establish voltage at their output as they work as a voltage source. Inside the cascaded control structure of the GFM converter, the magnitude of voltage along with its angle at the PCC is controlled dynamically so that the grid may be synchronized with the controller and supported as needed. Usually, if the ratio X/R of the grid is high, active power is associated with the frequency because the ratio X/R dictates the association between the active and reactive power, frequency, and voltage. Therefore, the controller for active power controls frequency/phase and the controller for reactive power controls the magnitude of the voltage at the PCC. Whereas, if the ratio X/R is less the reactive power and the frequency is associated. In this case, the opposite happens and the controller for active power now has to control the voltage magnitude and the controller for reactive power controls the frequency. The control methods can be characterized into three types as shown in Fig. 2. From Fig. 2. it can be seen that the first type is the synchronous machine-based control, the second type is the droop-based control and the other types of control are given in the third type. These three types are further divided based on the type of control method used. The synchronous machine-based control method contains the swing equation emulation, matching control, augmented virtual synchronous machine control, VISMA and synchronverter. The droop-based control method contains frequency-based droop control, power synchronization control and angle-based droop control. Other methods include virtual oscillator-based control, ViSynch, frequency shaping based control and H_∞ based control. The most widely used control technique among all these is the droop-based control. Some of the methods named above are discussed in the following subsections.

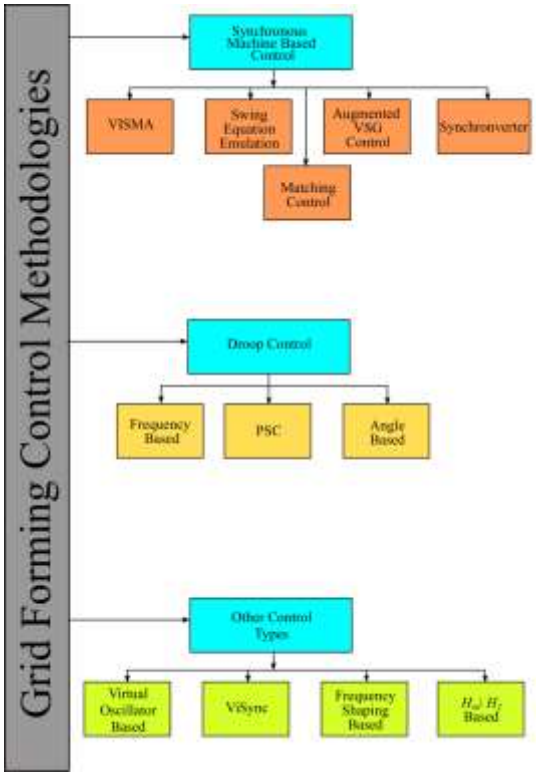

Fig. 2. Hierarchy of the control system

2.2. Droop Based Control

Out of the three talked about control techniques in this paper, droop control is extremely widespread and matured. Droop control is based on the governor action, which allows the working of several synchronous generators in parallel. Depending on the control technique, droop control can be classified into frequency-based, angle-based, and power synchronization control (PSC).

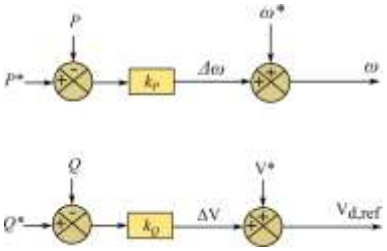

Fig. 3. Basic structure of droop control

2.2.1 Droop Control Based on Frequency

In this type of control technique, the frequency of the converter is decreased linearly with the increase in active power. Similarly, a voltage control mechanism could also be used to regulate the magnitude of voltage based on reactive power. The linear relation between frequency and active power is represented by the droop coefficient. This droop coefficient is selected in such a way that the load is shared among the converter based on their rating, in a standalone system [21].

Fig. 3 shows the control structure of the basic droop controller. Here, the droop coefficients are given as K_P and

K_Q. These droop coefficients are selected in such a way that while operating in a standalone mode the converters share the load depending upon their operation and rating. GFM converters controlled by droop can be deployed both in grid connected mode and standalone mode, controlling multiple GFM converters and GFL converters. The controllers can be implemented fairly easily, and redundancy can be achieved very easily [22].

2.2.2 Angle Based Droop

Droop control based on the angle is given in [23]. In this technique, the droop coefficients are chosen depending on the regulation of voltage and sharing of the load. In [24] a novel flux-based droop control is presented to overcome the problems in the traditional droop control based on voltage. Both the powers active and reactive are regulated by the magnitude of flux and the angle of the flux, respectively. Rather than the magnitude and phase angle of the voltage, the flux magnitude and flux angle are drooped in this technique.

2.2.3 Power Synchronization Control

Power Synchronization control (PSC) for HVDC systems is presented in [25]. In PSC, the phase angle is used for droop depending on the power increment instead of the frequency. The droop coefficient becomes Kθ. This overcomes the problems created by using inverters controlled by vector current in weak grids. Although, a PLL is not essential for the synchronization in a PSC, but, during faults, a PLL is utilized as a backup to switch to a GFL converter control.

2.3. Synchronous Machine Based Control

Despite the many advantages of droop controllers, one of the major shortcomings is the absence of inertia support. In order to eliminate this weakness, novel control methodologies that make use of the properties of synchronous generators like inertial and damping, are proposed.

2.3.1 Virtual Synchronous Machine

Synchronous generator behavior using power electronic components was emulated first by [26] as a virtual synchronous machine. On the basis of the measured voltage at the PCC, the currents of the machine are calculated in real time and injected into the grid. Both the powers active and reactive are regulated utilizing virtual torque and virtual excitation, respectively.

2.3.2 Swing Equation Emulation

The block diagram of control for the basic VSG is shown in Fig. 4. One major advantage of the VSG over synchronous machines is the ability to change certain design parameters such as DP and J during operation. Where DP is the damping constant and the moment of inertia is given as J.

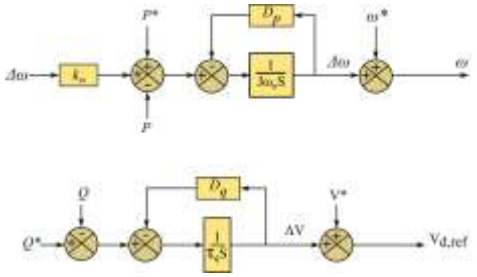

Fig. 4. Virtual synchronous machine control

In [27] a complete analysis of the droop control and VSG control is done. The authors considered both GFM converter's modes of operation i.e. grid connected and standalone for both VSG control and droop control. The system frequency changed during connection and disconnection of load. It was seen that due to the absence of inertia in the standalone mode the frequency rate of change was very high for the droop control in contrast to that of other control in comparison. This results in unwanted load shedding and tripping of the system. Moreover, the governor delay using droop control increased inertia.

2.3.3 Matching Control

By using the DC link voltage not merely as an essential signal of control but as well as a substitute signal for the imbalance in power, authors in [28], [29] have developed a unique GFM control method known as matching control which matches the electromechanical transfer of synchronous machine's energy. The block diagram is shown in Fig. 5. Reference [30] proposed the control technique built on energy shaping method and a comprehensive electronic understanding of synchronous machine. As opposed to a simulation of synchronous machine based on numerical simulation, the authors presented an accurate physical understanding of the machine by using the integral of DC bus voltage measurement to estimate the voltage source inverter's internal angular frequency. For this reason, they are equivalent to similar physical quantities of voltage source converter for instance moment of inertia and rotor damping coefficient.

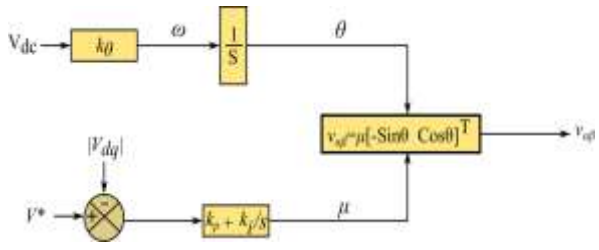

Fig. 5. Matching control block diagram

2.4. Other Control Types

There are many other different controls proposed for GFM converters besides conventional droop control and control based on synchronous machine. Some are linear control techniques, while the majority are nonlinear control techniques.

2.4.1. Virtual Oscillator Based Control

Control of the inverters via virtual oscillator control (VOC) matches the dynamics of a weak nonlinear oscillator with nonlinear control was presented in [31]. VOC is implemented using the converter current and voltage of capacitor. A control signal from the capacitor voltage is used in pulse width modulation (PWM) to build the voltage at the terminals. Inverters connected in parallel can synchronize with each other without needing any communication between them, which is one of the important cons of a VOC. Using previous work on VOC, researchers in [32], [33] have built a system that obtains the set points of power and voltage and drives the system of electrical power to the desired power output result as a replacement for an insignificant one, it is called dispatchable VOCs (dVOCs).

3 Model Description

3.1 The Control System of Voltage Source Converter

The layout of a voltage source converter system is shown in Fig. 6. It contains switching valves based on IGBTs or MOSFETs, a coupling reactor, a shunt filter, and a transformer. A coupling reactor is required to regulate the active and reactive power flow separately and to limit the short circuit current. A shunt filter is also necessary if the converter has two or three level topology. Together with the series reactor, the shunt filter removes the harmonics from the converter output voltage. A conventional two winding transformer is typically installed in the converter substation to match the point of common coupling (PCC) voltages.

The fundamental principle of active and reactive power flow control is based on equations (1) and (2). According to the equation, by controlling the difference between PCC and VSC bus voltage angles, active power (P) can be controlled, and by controlling the difference between PCC and VSC bus voltage magnitudes (Q), reactive power can be controlled. Here, l is the inductance of the series reactor and ω is the network frequency. It is considered that the series resistance r is very small and negligible.

$$P = \frac{V_{pcc}V_{vsc}\sin\Delta\delta}{\omega l} \quad (1)$$

$$Q = \frac{1}{\omega l}\{V_{vsc}^2 - V_{pcc}V_{vsc}\cos\Delta\delta\} \quad (2)$$

A voltage source converter can work in grid connected mode or grid forming mode. In the former mode, converter is synchronized with the frequency of the grid and it supports four operational control modes i.e., to control active power (P), to control reactive power (Q), to control DC voltage V_{dc}, and to control AC voltage V_{ac}. The reference frequency and the voltage are controlled by the main grid and the converter is synchronized with it using a phase locked loop (PLL) system. In the latter mode, the converter controls the frequency of the network and AC voltage to energize the isolated network.

As shown in Fig. 6, the designing of the control system is done in a balanced voltage synchronous rotating frame (dq0), commonly known as the vector control method. In vector control method, time variant three phase AC signal is transformed into time invariant signals so that the control system can be designed in a complex plane. For the balance system, the d-component corresponds to the real part, and q-component of the signal corresponds to an imaginary part, whereas the third component is always zero. Thus, AC network can be represented by phasor quantity. VSC converter control system has two main control loops connected in cascaded i.e., primary control and secondary control. The former mentioned control is mainly a current control loop that has a fast response time. Secondary control is either the power or voltage control loop and has a slow response time compared to primary control. From the modeling viewpoint, a voltage

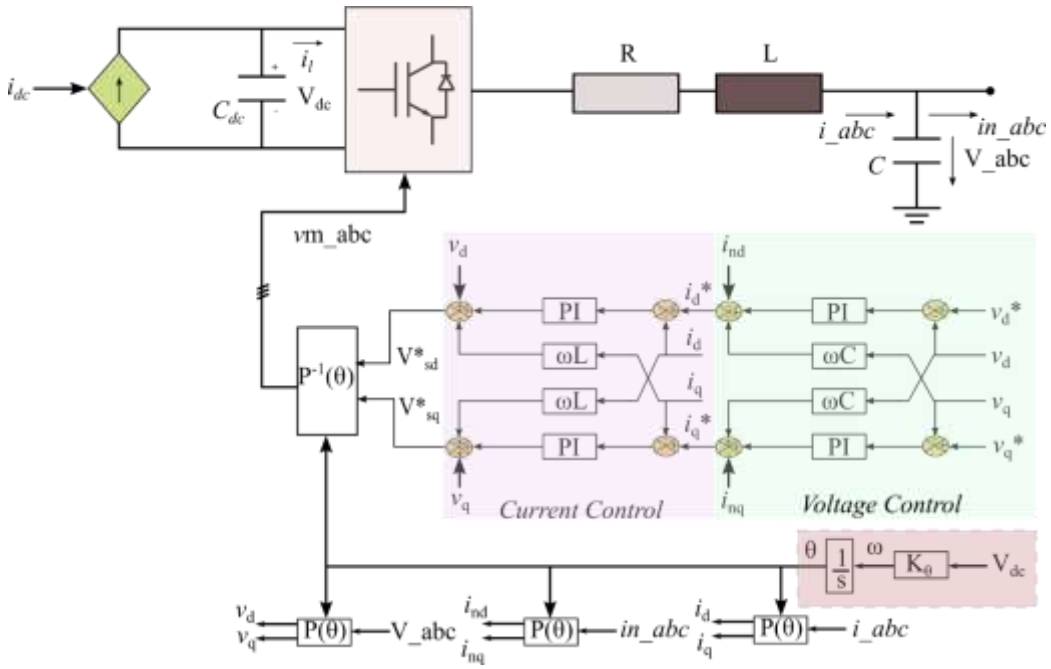

Fig. 6. Proposed control block diagram

source converter can be modeled as a controlled voltage source behind the series impedance. The inner current controller generates the voltage signal the dq-component of the reference voltage signal which can be then transformed into an abc-system using Clarke transform and the Park transform to generate the switching pattern of the IGBTs or MOSFETs.

3.2 Detailed Description of the Proposed Control System

The proposed control system overview is shown in Fig. 6. An inner current control system and an outer voltage control system are part of the control system. The angle reference for all dq0 components of current and voltage is generated by the control structure depending on the DC link voltage as shown in Fig. 6.

3.2.1 Inner Current Control

The dynamic behavior of current flowing through the series reactor can be expressed using equations (3) and (4). The system equation shows that the current d- and q-components are coupled together and it is a multi-input-multi-output system. This means that the change in the current d-component reference command will affect the current q-component that will flow through the series reactor. The decoupling scheme can be applied to independently control both current components. Consequently, active and reactive power flow through the VSC can be controlled independently of each other.

$$\begin{bmatrix} v_{sd}^* \\ v_{sq}^* \end{bmatrix} = \begin{bmatrix} v_d \\ v_q \end{bmatrix} + \begin{bmatrix} 0 & -\omega l \\ \omega l & 0 \end{bmatrix} \begin{bmatrix} i_d \\ i_q \end{bmatrix} + \begin{bmatrix} v_{cd} \\ v_{cq} \end{bmatrix} \quad (3)$$

$$\begin{bmatrix} v_{cd} \\ v_{cq} \end{bmatrix} = \begin{bmatrix} r & 0 \\ 0 & r \end{bmatrix} \begin{bmatrix} i_d \\ i_q \end{bmatrix} + \begin{bmatrix} l & 0 \\ 0 & l \end{bmatrix} \frac{d}{dt} \begin{bmatrix} i_d \\ i_q \end{bmatrix} \quad (4)$$

Here, v_{cd} and v_{cq} are the control signal generated by the inner current controller. ω is the network frequency. v_d and v_q are the dq-component of controlling bus voltage which is typically are capacitor bus as shown in Fig. 7. i_d and i_q are the current component flowing through the reactor. v_{sd}^* and v_{sq}^* are the generated voltage at the converter busbar.

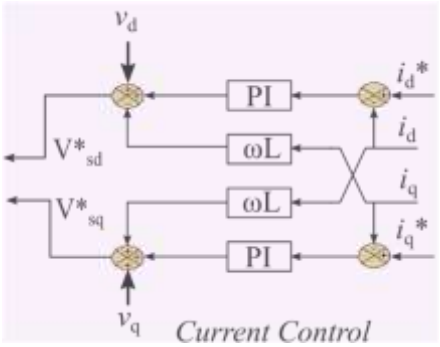

Fig. 7. Inner current control

Proportional integral (PI) controller is chosen to achieve the zero steady state error for tracking the reference current command. The closed loop control analysis can be performed using equations (3) and (4). The controller gain can be calculated using equation (5) by applying internal model control (IMC) method.

$$k_p = \frac{l}{\tau_i}, k_i = \frac{r}{\tau_i} \quad (5)$$

Here, r is the series reactor's resistance, l is the inductance, τ_i is the required time constant of the loop that controls current. Proportional and integral gains are given by k_p and k_i respectively.

3.2.2 Outer Voltage Control

In grid forming mode, the reference current command for primary control loop is generated by secondary controller which controls the voltage at the filter busbar connected in shunt. The dynamic behavior of voltage across the filter capacitor can be expressed by equations (6) and (7). It can be observed from equations (6) and (7) that the voltage d- and q-components are coupled with each other. A decoupling scheme can be applied as shown in Fig. 8 to control the voltage dq-component independently.

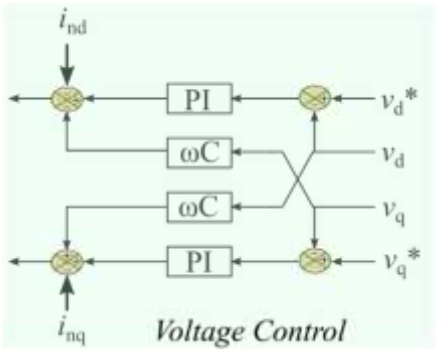

Fig. 8. Outer voltage control

$$\begin{bmatrix} i_d^* \\ i_q^* \end{bmatrix} = \begin{bmatrix} i_{nd} \\ i_{nq} \end{bmatrix} + \begin{bmatrix} 0 & -\omega c \\ \omega c & 0 \end{bmatrix} \begin{bmatrix} v_d \\ v_q \end{bmatrix} + \begin{bmatrix} i_{cd} \\ i_{cq} \end{bmatrix} \quad (6)$$

$$\begin{bmatrix} i_{cd} \\ i_{cq} \end{bmatrix} = \begin{bmatrix} c & 0 \\ 0 & c \end{bmatrix} \frac{d}{dt} \begin{bmatrix} v_d \\ v_q \end{bmatrix} \quad (7)$$

Here, i_{cd} and i_{cq} are the outer voltage controller output signal, i_{nd} and i_{nq} are the load current, capacitance of the filter is given by c, and i_d^* and i_q^* are the command of reference for the inner current controller.

3.3 Mathematics of the Proposed Control System

The block diagram of the proposed control is shown in Fig. 6. The idea was developed by observing that the DC-link voltage can imply power imbalances similar to a synchronous machine frequency. To drive the converter frequency, the DC voltage, up to a certain constant factor, is used. The phase angle is given by

$$\theta = K_\theta v_{dc} \quad (8)$$

Where, $K_\theta = \frac{\omega}{v_{dc}}$ and ω is the reference frequency and v^*_{dc} is the nominal dc voltage.

From Fig. 6 it can be seen

$$C_{dc} v_{dc} = i_{dc} - i_l \quad (9)$$

Where i_{dc} is the source current and i_l is the current input to the converter. To control the voltage of DC link the DC current reference i_{dc} is given by a proportional control

$$i_{dc} = k_{dc}(v_{dc}^{*} - v_{dc}) \quad (10)$$

To explain the concept of proposed control more, we replace v_{dc} in equation (9) with ω/K_θ in equation (11). This results in

$$\theta = \omega \quad (11)$$

$$C_{dc}\omega = K_\theta i_{dc} - K_\theta i_l \quad (12)$$

The synchronous machine's angle and frequency dynamics are given by [34].

$$\theta = \omega \quad (13)$$

$$J\omega = T_m - T_e \quad (14)$$

Comparing equation (12) and equation (14) reveals the structural similarities of the proposed control to that of a synchronous machine. Dividing equation (12) by K_θ^2 to acquire the similar units as in equation (14) and matching the variables with (14) gives us $J=C_{dc}/K_\theta^2$, $T_m=i_{dc}/K_\theta$ and $T_e=i_l/K_\theta$. To put it simply, the internal energy storage of a GFM converter is linked by the inertia constant. Furthermore, the frequency response is given by the proportional DC voltage control given in equation (10).

3.4 Model Description

A model of the system shown in Fig. 9, has been developed in MATLAB. The details of the model are given in Table 1. In this study, the GFM converter is an average model of two level VSC which is connected to a three phase transformer. The detailed derivation of the model is out of the scope of this paper. Four types of control are designed for the GFM converter. The model is simulated for all four types of controls and the results of frequency, power, and voltage are observed. The four types of controls which are simulated are droop, VSM, matching, and proposed control. The converter is attached to a transformer that is connected to a load. This model validates the working of the proposed control and compares the result with other GFM control strategies.

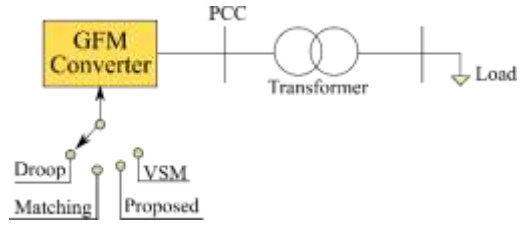

Fig. 9. System model

Table 1. Model description and system parameters

Base Values of System		**GFM Transformer**	
S_{base}	112 MVA	V_1	75 kV
V_{base}	33 kV	V_2	33 kV
ω_{base}	2π50 rad/s	R_1=R_2	4 %
VSM		**Droop**	
D_p	10^5	d_ω	2π0.05
J	2000	ω	2π50
K_p	0.001	K_p	0.001
Matching		**AC DC Voltage Control**	
K_θ	0.12	K_{pv}	0.52
K_{dc}	$1.6x10^3$	K_{iv}	232.2
K_p	0.001	K_{pi}	0.73
Proposed Control		**Parameters**	
K_θ	0.0021	AC filter Capacitance GFM/GFL	2.631/- (μF)
K_{pv}	70	Reactor Resistance GFM/GFL	0.0363/0.0001(Ω)
K_{iv}	700	Reactor Inductance GFM/GFL	55/0.02 (mH)
K_{pi}	120	Network Frequency	50 Hz
K_{ii}	1500	GFL WT rating	6.3 MVA
K_{dc}	0.4977	GFL WT Transformer	0.9/33 kV
		V_{dc}	±150 kV

4. Simulation Results

The nonlinear simulation results performed in MATLAB/Simulink are presented in this section to verify the control proposed in section three. Table 1 presents the parameters used in the simulation. The simulation tests the dynamic characteristic of the converter during network current change and power step. The steady state operation characteristics of the system are presented.

4.1 Dynamic Characteristics of the Converter During Network Current Change

The system is energized and a power increase of 0.22 p.u. is applied at t= 25 s. The system is tested for changes in frequency, voltage, and power for all types of controls. Fig. 11 shows the change in frequency of the GFM converter. As can be seen from Fig. 10 that the frequency is decreased with an increase in the power. Droop control and VSM control synchronize with the system easily while the matching control overshoots and then synchronize after a lot of oscillations. In the proposed control there is a noticeable oscillation in the system which can be seen in Fig. 11 but, unlike the matching control, the system remains stable during the network current change.

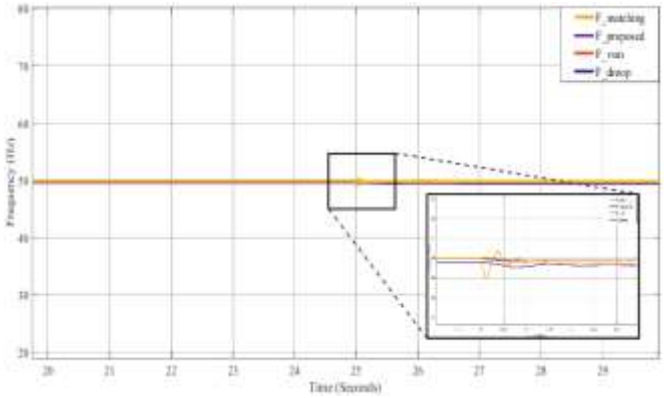

Fig. 10. Nonlinear simulation result of frequency with different types of grid forming control

Similarly, the behavior of power is shown in Fig. 11. The power is increased slightly above the given set value and then comes back to the set value for all other controls. The droop control value is higher among the other controls. From Fig. 11 it can be seen that the power does not increase for the proposed control and remained at the set value even after an increase of power.

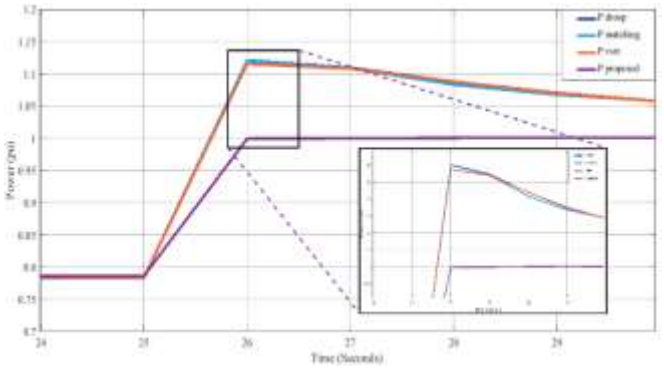

Fig. 11. Nonlinear simulation result of power with different types of grid forming control

The behavior of voltage is seen in Fig. 12. The voltage remains within the permissible range and not much difference is seen by increasing the active power set point. This is due to the fact that the magnitude of the voltage is linked with the reactive power.

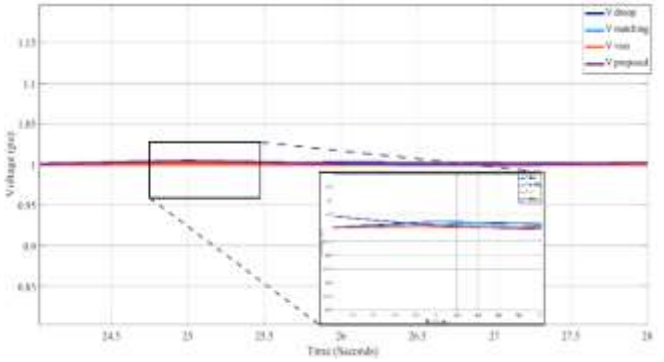

Fig. 12. Nonlinear simulation result of voltage with different types of grid forming control

4.2 Performance of the converter in response to a load disturbance

To check the performance of the converter with the proposed control a test case is simulated using MATLAB/Simulink. The power is stepped up from 0.45 p.u. to 1 p.u. at t= 1.5 s. With an increase in the load of this category, the system frequency should decrease a lot. But as can be seen from Fig. 13 the frequency is controlled within the permissible range with very slight oscillation. The system remains stable and the power is transferred from the converter to the load.

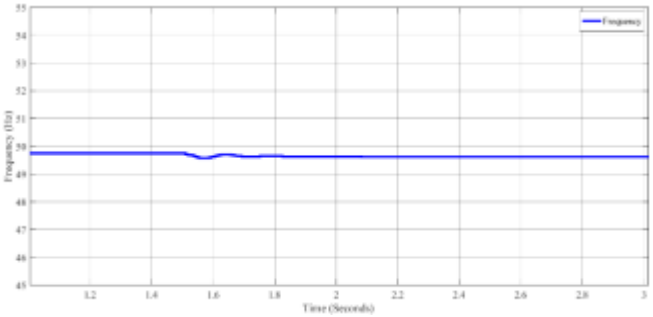

Fig. 13. Frequency of the system

The active power change is shown in Fig. 14, the power is stepped up from 0.45 p.u. to 1 p.u. It is observed from the figure that an increase in power does not destabilize the system and the power is transferred to the load. The converter is supplying a power of 0.45 p.u. and at t= 1.5 s the power is increased to 1 p.u. The converter without affecting other parameters of the system starts supplying the power as can be seen.

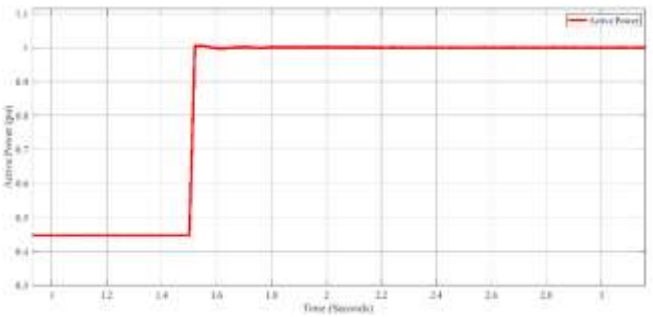

Fig. 14. Large load disturbance power increased from 0.45 p.u. to 1 p.u.

The performance of the system for this load disturbance is shown in Fig. 15 in terms of the three-phase voltage and current profile of the system. The converter voltage along with the filter voltage is stable and remain stable after the load change. The load voltage is stable and the grid current can be seen increasing from 0.45 p.u. to 1 p.u. for a similar load change. This shows that the converter is supplying power to the load and the system quickly adjusts itself by increasing the current to the new load value that is 1 p.u.

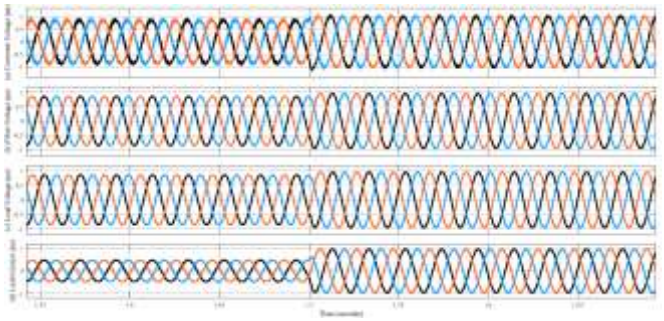

Fig. 15. Performance of the overall system

Figure 16 shows the voltage in per unit of the load. The voltage does not show any significant variation after the load change. Only a small spike downwards can be seen at the time of load increase which is in the permissible range. The voltage is not much affected by the active power as it is linked to the reactive power change.

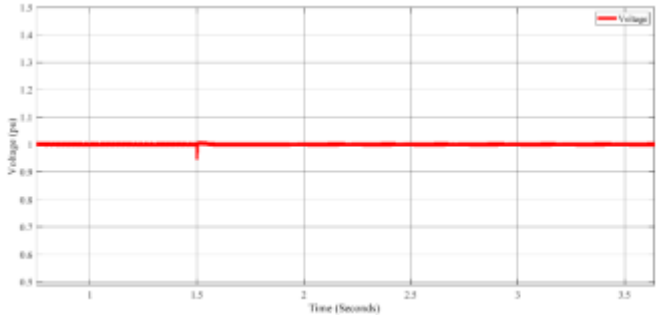

Fig. 16. Voltage of the system

The proposed control also controls the DC voltage of the link behind the converter. The DC voltage profile is shown in Fig. 17. It is shown that at the time of load change the DC link voltage is reduced very slightly and then comes back to its rated value. The frequency response in the proposed control is provided by the DC link voltage and the change in power system. The nonlinear dynamic simulation shown in Fig. 17 validates the working of the proposed controller as it stabilizes the DC link voltage.

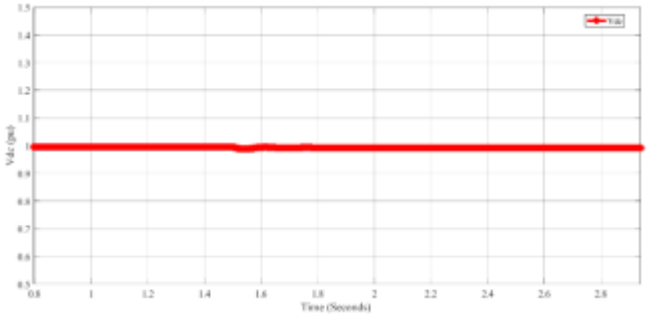

Fig. 18. DC voltage of the converter

4.3 Proposed Control Technique in Hybrid HVDC System

In order to test the proposed control in the hybrid HVDC system shown in Fig. 18, the simulation was performed in MATLAB/Simulink environment. The offshore substation uses DR as an electronic converter for the conversion of power. It consists of uncontrolled 12 pulse DRs connected in series for the conversion and filter banks and reactive power for compensation. The system parameters are given in Table 1. The VSC was implemented using an average value model whereas the diode rectifier was implemented using a switching model. The grid forming converter was implemented in the same way as discussed in the above section and the grid following wind turbines were synchronized with the grid using a PLL [35-40]. The oversimplification of the dynamics of the wind turbines was enough to prove the concept of hybrid HVDC system and the parallel operation of the grid forming wind turbine with the grid following wind turbines.

The grid forming wind turbine was enabled at t= 0 s, establishing the offshore grid and exporting the power towards the onshore grid. The sequence is given in Table 2.

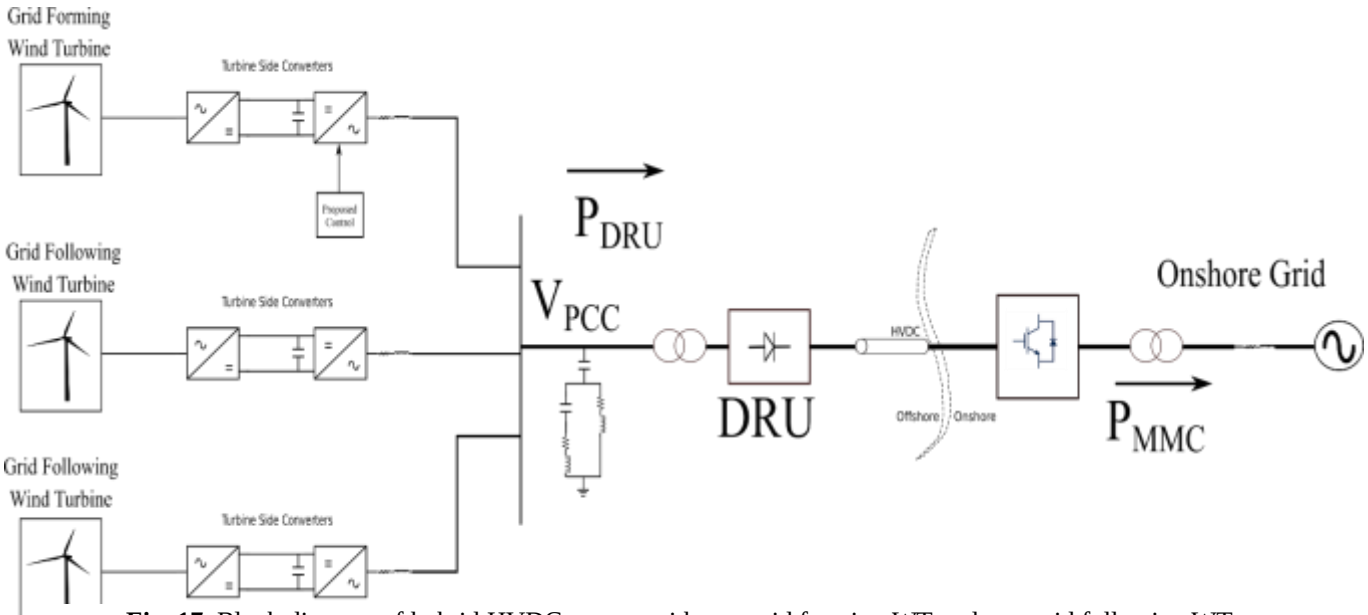

Fig. 17. Block diagram of hybrid HVDC system with one grid forming WT and two grid following WTs

disturbs the DC voltage slightly without destabilizing the

Table 2. Sequence of events

Time	Events
0 s	The grid forming wind turbine is started and offshore substation is established.
1 s	Grid following wind turbine one is connected to the system and it starts injecting power.
1.7 s	The second grid following wind turbine is connected to the system and it starts injecting power.

In Fig. 19 at t= 0 s the offshore grid forming WT was enabled which established the offshore grid and started injecting power. At t= 1 s the first grid following WT was connected at the PCC with the offshore substation, which followed the already established offshore grid using PLL and started injecting power into the grid. At t= 1.7 s the second WT was connected to the system which followed the same procedure as the first WT. Fig. 19 (a) shows the total power injected by the offshore wind farm in which the power is increased at t= 1 s and t= 1.7 s when the grid following WT are connected. Fig. 19 (b) shows the voltage of the PCC in per unit. The voltage has noticeable oscillations, but they are in the permissible region
and the system remains stable. This can be confirmed from Fig. 19 (c) in which the frequency remains in the permitted range and with very low oscillations. Clearly, the system is stable when the grid following WTs are connected. Fig. 19 (d) and 19 (e) show the three-phase voltage and current at the PCC.

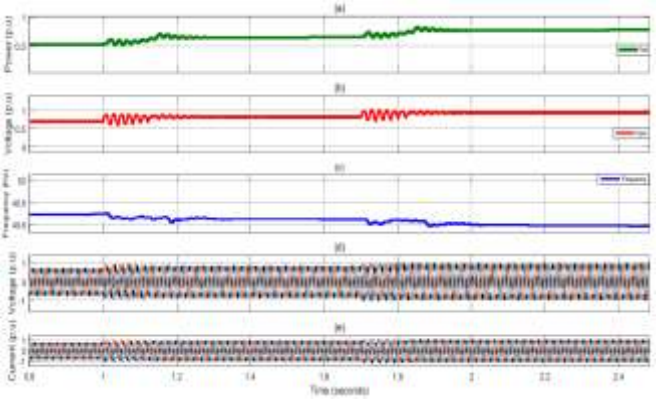

Fig. 19. Nonlinear simulation result of (a) Power at PCC (b) Voltage at PCC (c) Frequency at PCC (d) Three phase voltage at PCC (e) Three phase current at PCC

Fig. 20 shows the dynamics of the grid following wind turbines. The current and power of both the wind turbines are zero before connection. After the connection is made both the WTs start injecting power and the current can be seen flowing. Fig. 20 (a) and 20 (b) show the dynamics of WT one while Fig. 20 (c) and 20 (d) show the dynamics of WT two.

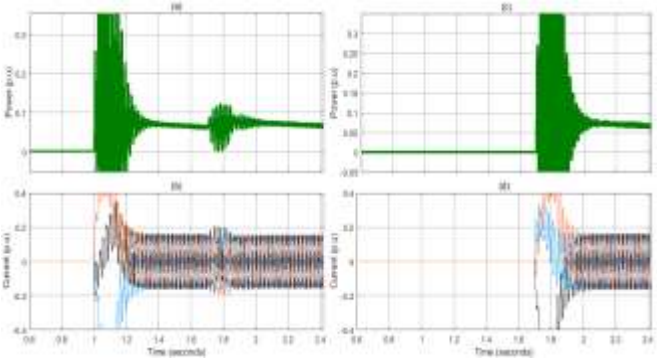

Fig. 20. Power and current of Grid following wind turbines (a) Power of WT 1 (b) Current of WT 1 (c) Power of WT 2 (d) Current of WT 2

Table 3. Comparison with other control techniques

Control Technique	PLL for synchronization	Communication less	Virtual inertia	Remarks
Droop	✓	×†	✓	Still require investigation in hybrid HVDC system based on DRU.
VSM	✓	✓	✓	It requires PLL for synchronization which limits its use in hybrid HVDC system.
Matching	×	✓	✓	When used in DRU based HVDC system the system is unable to keep frequency within permissible range.
Proposed	×	✓	✓	The proposed control works well in hybrid HVDC system, establishing the grid for other WTs to follow. The use of no PLL makes the system more robust.

† In the angle-based droop control GPS is required to obtain the angle reference. Other droop strategies like frequency based and PSC does not require communication.

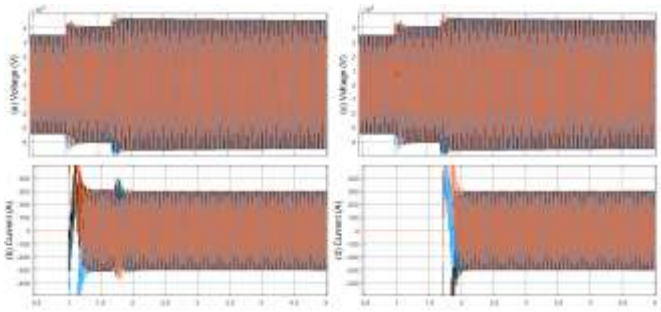

Fig. 21. Voltage and current of Grid following wind turbines in RMS (a) Voltage of WT 1 (b) Current of WT 1 (c) Voltage of WT 2 (d) Current of WT 2

Fig. 21 shows the three-phase voltage and current of the grid following wind turbines in RMS. It can be observed from Fig. 21(b) and Fig. 21(d)that when the wind turbine one is connected to the PCC at t= 1 s the current starts to flow. Similarly, for wind turbine two, the current starts to flow at t= 1.7 s i.e. when it is connected to the PCC. The three-phase voltage of the PCC in RMS is shown in Fig. 21(a) and Fig. 21(c).

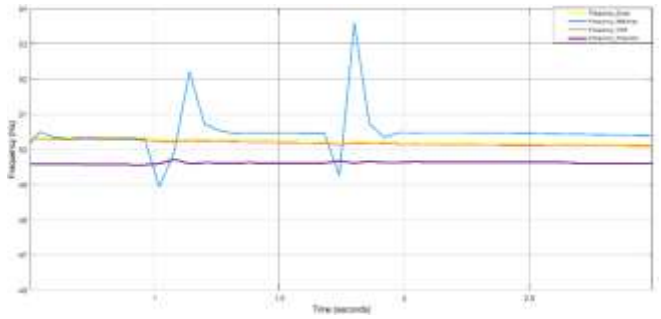

Fig. 22. Comparison of system frequency with different control techniques

Fig. 22 shows the comparison of the frequency of the system with other control strategies. At t= 1 s wind turbine one is connected and at t= 1.7 s wind turbine two is connected. The connection of the wind turbine introduces transient in the system which the proposed control handles pretty well similar to the droop and VSM control techniques but the matching control exceeds the permissible frequency limit and hence destabilizes the system. This shows that the proposed control can be used in offshore wind farms and can give similar performance as other control strategies.

Table 3 shows the comparison of different grid forming control techniques with the proposed control. The VSM technique require PLL for synchronization whereas the matching control and the proposed control do not require PLL for synchronization and work well without the PLL. Almost all the methods are without communication except for the droop technique based on angle, as it requires GPS to obtain the angle. Virtual inertia is present in all control methods. In contrast to the control technique present in [5], the proposed control scheme is decentralized and high-speed communication is not needed because it involves only local measurements. The grid forming wind turbine establishes the grid using only the local measurements, which other wind turbines follow to connect and inject the power. The proposed control itself does not require PLL making the system more robust. The communication is needed by other grid following wind turbines to follow and connect with the grid established by the grid forming wind turbine.

5. Conclusion

Grid forming converters have emerged as an exciting and promising solution for the problems related to weak grids. It is observed through the review of literature that advanced research is required to set up the offshore network using grid forming control in a hybrid HVDC system. The existing wind turbines are unable to establish the offshore network and are unable to black start an offshore wind farm in a hybrid HVDC system. This article presents a new grid forming control structure to establish the offshore network in offshore wind farms based on a hybrid HVDC system. To evaluate the performance of the proposed control, a study has been conducted. Under several different conditions, the proposed grid forming control is observed to provide comparable performance. This paper also reveals that the proposed grid forming converter control can be used in an offshore wind farm successfully and other grid following wind turbines can connect to the offshore grid established by the grid forming converter to inject power. The areas which require further research are also highlighted in this paper.

APPENDIX

The values for the following parameters were calculated as below [41].

$$K_\theta = \frac{\omega}{v_{dc}}$$

$$K_{dc} = \frac{\omega S_{base}}{{V_{dc}}^2 (2\pi 0.5)}$$

Table I. Variables in Equations

Variable name	Variable
P	Active power
Q	Reactive power
ω	Network frequency
V_{pcc}	Voltage magnitude of PCC
V_{vsc}	Voltage magnitude of VSC
v_{sd}^*, v_{sq}^*	The generated voltage at the converter busbar
v_d, v_q	dq-component of controlling bus voltage which is typically are capacitor bus
v_{cd}, v_{cq}	Control signal generated by the inner current controller
i_d, i_q	Current components flowing through the reactor
i_d^*, i_q^*	Reference commands for inner current controller
i_{nd}, i_{nq}	Load currents
i_{cd}, i_{cq}	Voltage controller output signal
v_{dc}	DC link voltage
v^*_{dc}	Nominal dc voltage
C_{dc}	DC link capacitance
i_{dc}	Source current
i_l	Current input to the converter
J	Moment of inertia
T_m & T_e	Mechanical and Eletromagnetic torque

References

[1] G. Guo, Q. Song, B. Zhao, H. Rao, S. Xu, Z. Zhu and W. Liu, "Series-connected-based offshore wind farms with full-bridge modular multilevel converter as grid- and generator-side converters," *IEEE Transactions on Industrial Electronics*, vol. 67, pp. 2798-2809, 2019.

[2] N. B. Negra, J. Todorovic and T. Ackermann, "Loss evaluation of HVAC and HVDC transmission solutions for large offshore wind farms," *Electric power systems research*, vol. 76, pp. 916-927, 2006.

[3] A. E. Leon, "Short-term frequency regulation and inertia emulation using an MMC-based MTDC system," *IEEE Transactions on Power Systems*, vol. 33, pp. 2854-2863, 2017.

[4] A. Bidadfar, O. Saborío-Romano, N. A. Cutululis and P. E. Sørensen, "Control of offshore wind turbines connected to diode-rectifier-based HVdc systems," *IEEE Transactions on Sustainable Energy*, vol. 12, pp. 514-523, 2020.

[5] R. Blasco-Gimenez, S. Ano-Villalba, J. Rodríguez-D'Derlée, F. Morant and S. Bernal-Perez, "Distributed voltage and frequency control of offshore wind farms connected with a diode-based HVdc link," *IEEE Transactions on Power Electronics*, vol. 25, pp. 3095-3105, 2010.

[6] O. Saborío-Romano, A. Bidadfar, J. N. Sakamuri, Ö. Göksu and N. A. Cutululis, "Novel energisation method for offshore wind farms connected to HVdc via diode rectifiers," in *IECON 2019-45th Annual Conference of the IEEE Industrial Electronics Society*, 2019.

[7] Y. Chang and X. Cai, "Hybrid topology of a diode-rectifier-based HVDC system for offshore wind farms," *IEEE Journal of Emerging and Selected Topics in Power Electronics*, vol. 7, pp. 2116-2128, 2018.

[8] R. Ramachandran, S. Poullain, A. Benchaib, S. Bacha and B. Francois, "On the Black Start of Offshore Wind Power Plants with Diode Rectifier based HVDC Transmission," in *2019 21st European Conference on Power Electronics and Applications (EPE'19 ECCE Europe)*, 2019.

[9] J. Li, J. Yin, Y. Guan, Z. Wang, T. Niu, H. Zhen, Z. Han and X. Guo, "A Review on Topology, Operating and Control Methods of HVDC Transmission System for Offshore Wind Farms," in *E3S Web of Conferences*, 2020.

[10] A. Nami, J. L. Rodriguez-Amenedo, S. Arnaltes, M. Á. Cardiel-Álvarez and R. A. Baraciarte, "Frequency Control of Offshore Wind Farm With Diode-Rectifier-based HVdc Connection," *IEEE Transactions on Energy Conversion*, vol. 35, pp. 130-138, 2019.

[11] R. Rosso, X. Wang, M. Liserre, X. Lu, and S. Engelken, "Gridforming converters: Control approaches, grid-synchronization, and future trends—a review," *IEEE Open Journal of Industry Applications*, vol. 2, pp. 93–109, 2021.

[12] C. Yang, L. Huang, H. Xin, and P. Ju, "Placing grid-forming converters to enhance small signal stability of pll-integrated power systems," *IEEE Transactions on Power Systems*, vol. 36, no. 4, pp. 3563–3573, 2021

[13] A. Roscoe, T. Knueppel, R. Da Silva, P. Brogan, I. Gutierrez, D. Elliott, and J.-C. Perez Campion, "Response of a grid forming wind farm to system events, and the impact of external and internal damping," *IET Renewable Power Generation*, vol. 14, no. 19, pp. 3908–3917, 2020.

[14] A. Roscoe, P. Brogan, D. Elliott, T. Knueppel, I. Gutierrez, J. Perez Campion, and R. Da Silva, "Practical experience of operating a grid forming wind park and its response to system events*," in Proceeding of the 18th Wind Integration Workshop*, Dublin, Ireland, 2019, pp. 16–18.

[15] C. Prignitz, H.-G. Eckel, S. Achenbach, F. Augsburger and A. Schön, "FixReF: A control strategy for offshore wind farms with different wind turbine types and diode rectifier HVDC transmission," in *2016 IEEE 7th*

International Symposium on Power Electronics for Distributed Generation Systems (PEDG), 2016.

[16] L. Yu, R. Li and L. Xu, "Distributed PLL-based control of offshore wind turbines connected with diode-rectifier-based HVDC systems," *IEEE Transactions on Power Delivery*, vol. 33, pp. 1328-1336, 2017.

[17] N. G. Khani, M. Abedi, G. B. Gharehpetian, and G. H. Riahy, "Offshore wind farm power control using HVDC link," *Canadian Journal of Electrical and Computer Engineering*, vol. 39, no. 2, pp. 168-173, 2016.

[18] A. Jain, J. N. Sakamuri and N. A. Cutululis, "Grid-forming control strategies for black start by offshore wind power plants," *Wind Energy Science*, vol. 5, pp. 1297-1313, 2020.

[19] J. Rocabert, A. Luna, F. Blaabjerg and P. Rodriguez, "Control of power converters in AC microgrids," *IEEE transactions on power electronics*, vol. 27, pp. 4734-4749, 2012.

[20] H. Shahinzadeh, A. Gheiratmand, J. Moradi, and S. H. Fathi, "Simultaneous operation of near-to-sea and offshore wind farms with ocean renewable energy storage," *in 2016 Iranian Conference on Renewable Energy & Distributed Generation (ICREDG)*. IEEE, 2016, pp. 38-44.

[21] H. Han, X. Hou, J. Yang, J. Wu, M. Su and J. M. Guerrero, "Review of power sharing control strategies for islanding operation of AC microgrids," *IEEE Transactions on Smart Grid*, vol. 7, pp. 200-215, 2015.

[22] T. L. Vandoorn, J. D. M. De Kooning, B. Meersman and L. Vandevelde, "Review of primary control strategies for islanded microgrids with power-electronic interfaces," *Renewable and Sustainable Energy Reviews*, vol. 19, pp. 613-628, 2013.

[23] R. Majumder, B. Chaudhuri, A. Ghosh, R. Majumder, G. Ledwich and F. Zare, "Improvement of stability and load sharing in an autonomous microgrid using supplementary droop control loop," *IEEE transactions on power systems*, vol. 25, pp. 796-808, 2009.

[24] J. Hu, J. Zhu, D. G. Dorrell and J. M. Guerrero, "Virtual flux droop method—A new control strategy of inverters in microgrids," *IEEE Transactions on Power Electronics*, vol. 29, pp. 4704-4711, 2013.

[25] L. Zhang, L. Harnefors and H.-P. Nee, "Power-synchronization control of grid-connected voltage-source converters," *IEEE Transactions on Power systems*, vol. 25, pp. 809-820, 2010.

[26] O. Mo, S. D'Arco and J. A. Suul, "Evaluation of virtual synchronous machines with dynamic or quasi-stationary machine models," *IEEE Transactions on industrial Electronics*, vol. 64, pp. 5952-5962, 2016.

[27] J. Liu, Y. Miura and T. Ise, "Comparison of dynamic characteristics between virtual synchronous generator and droop control in inverter-based distributed generators," *IEEE Transactions on Power Electronics*, vol. 31, pp. 3600-3611, 2015.

[28] T. Jouini, C. Arghir and F. Dörfler, "Grid-friendly matching of synchronous machines by tapping into the DC storage," *IFAC-PapersOnLine*, vol. 49, pp. 192-197, 2016.

[29] C. Arghir, T. Jouini and F. Dörfler, "Grid-forming control for power converters based on matching of synchronous machines," *Automatica*, vol. 95, pp. 273-282, 2018.

[30] C. Arghir and F. Dörfler, "The electronic realization of synchronous machines: Model matching, angle tracking, and energy shaping techniques," *IEEE Transactions on Power Electronics*, vol. 35, pp. 4398-4410, 2019.

[31] B. B. Johnson, S. V. Dhople, A. O. Hamadeh and P. T. Krein, "Synchronization of parallel single-phase inverters with virtual oscillator control," *IEEE Transactions on Power Electronics*, vol. 29, pp. 6124-6138, 2013.

[32] M. Colombino, D. Groß and F. Dörfler, "Global phase and voltage synchronization for power inverters: a decentralized consensus-inspired approach," in *2017 IEEE 56th Annual Conference on Decision and Control (CDC)*, 2017.

[33] M. Colombino, D. Groß, J.-S. Brouillon and F. Dörfler, "Global phase and magnitude synchronization of coupled oscillators with application to the control of grid-forming power inverters," *IEEE Transactions on Automatic Control*, vol. 64, pp. 4496-4511, 2019.

[34] P. Kundur, "Power system stability," *Power system stability and control*, vol. 10, McGraw-Hill, 2007.

[35] M. Raza, "Offshore grid control of voltage source converters for integrating offshore wind power plants," Universitat Politècnica de Catalunya, 2017.

[36] Allouche, Moez, Sahbi Abderrahim, H. Ben Zina, and Mohamed Chaabane. "A Novel fuzzy Control Strategy for Maximum Power Point Tracking of Wind Energy Conversion System." International Journal of Smart Grid-ijSmartGrid 3, no. 3 (2019): 120-127.

[37] Raza, Muhammad, and Oriol Gomis-Bellmunt. "Control system of voltage source converter to interconnect offshore ac hub with multiple onshore grids." In 2015 International Conference on Renewable Energy Research and Applications (ICRERA), pp. 677-682. IEEE, 2015.

[38] Simpson, Cameron, Agusti Egea Alvarez, and Maurizio Collu. "Influence of the Mission Profile on The Lifetime

Modelling of the Wind Turbine Power Converter–A Review." In 2020 9th International Conference on Renewable Energy Research and Application (ICRERA), pp. 144-151. IEEE, 2020.

[39] Oyegoke, Solomon, Marios Maniatopoulos, Simeon Keates, and Yehdego Habtay. "Frequency and voltage control of island system using power hardware in the loop." In 2019 8th International Conference on Renewable Energy Research and Applications (ICRERA), pp. 587-592. IEEE, 2019.

[40] Nagai, Satoshi, Kouki Tokui, Hiroki Watanabe, and Jun-Ichi Itoh. "Wind Turbine Generator Emulator with Current Control mode." In *2019 8th International*

[41] *Conference on Renewable Energy Research and Applications (ICRERA)*, pp. 733-738. IEEE, 2019.

A. Tayyebi, D. Groß, A. Anta, F. Kupzog and F. Dörfler, "Frequency stability of synchronous machines and grid-forming power converters," IEEE Journal of Emerging and Selected Topics in Power Electronics, vol. 8, pp. 1004-1018, 2020.